MultiCraft

International Journal of Engineering, Science and Technology
Vol. 6, No. 5, 2014, pp. 13-25

INTERNATIONAL JOURNAL OF ENGINEERING, SCIENCE AND TECHNOLOGY

www.ijest-ng.com
www.ajol.info/index.php/ijest

Chemical reaction on MHD flow and heat transfer of a nanofluid near the stagnation point over a permeable stretching surface with non-uniform heat source/sink

B. J. Gireesha[1] and N. G. Rudraswamy

Department of Studies and Research in Mathematics, Kuvempu University, Shankaraghatta-577 451, Shimoga, Karnataka, INDIA
[1]Corresponding Author: e-mail: bjgireesu@rediffmail.com Tel: 091+ 9741148002

Abstract

A numerical investigation has been conducted to study the laminar, boundary layer stagnation point flow of a nanofluid over a permeable, vertical stretching sheet. The model used incorporates the effects of Brownian motion with thermophoresis in the presence of uniform magnetic field and non-uniform source/sink under the influence of chemical reaction. Governing partial differential equations are transformed into a set of nonlinear ordinary differential equations using suitable similarity transformations. The transformed equations are then solved numerically using well known Runge-Kutta-Fehlberg method of fourth-fifth order with the help of symbolic software MAPLE. The influence of governing parameters on flow field, temperature and nanoparticle volume fraction profiles are provided both in graphical and tabular form. It is observed that heat source/sink with thermophoresis particle deposition in the presence of magnetic field have a substantial effect on the flow field and thus, on the heat and mass transfer rate from the sheet to the fluid. As the strength of the chemical reaction is higher than the thermophoresis particle deposition, nanoparticle volume fraction of the fluid gradually decreases. A comparative study has been conducted and is found to be in excellent agreement.

Keywords: Stagnation point flow; Chemical reaction; Heat transfer; Stretching surface; Nanofluid; Numerical solution.

DOI: http://dx.doi.org/10.4314/ijest.v6i5.2

1. Introduction

Nanofluid, a new class of heat transfer fluid that contains a mixture of nano particles or fibres in a base fluid. The use of additives is a technique applied to enhance the heat transfer performance of the base fluid. Choi (1995) coined the word nanofluid, as a fluid mixture comprising of nano particles or fibres, which initiated the studies on nanofluid. The theory of nanofluids has presented several fundamental properties with the large enhancement in thermal conductivity as compared to the basefluid (Fan and Wang, 2011). A large number of experimental and theoretical studies have been carried out by numerous researchers on thermal conductivity of nanofluids (Fan and Wang, 2011; Yoo et al., 2007a,b; Singh, 2008; Kleinstreuer and Feng, 2011). A phenomenon observed by Masuda et al. (1993) that characteristic feature of nanofluids is thermal conductivity enhancement. This phenomenon suggests the possibility of using nanofluids in advanced nuclear systems (Buongiorno and Hu, 2005). A comprehensive survey of convective transport in nanofluids was made by Buongiorno (2005), who says that a satisfactory explanation for the abnormal increase of the thermal conductivity and viscosity is yet to be found. He has focused on further heat transfer enhancement observed in convective situations.

The study of boundary layer flow and heat transfer over a stretching surface particularly in the field of nanofluid has achieved a lot of success in the past years because of its high thermal conductivity and large number of applications in industry and technology. Few of these applications are in manufacturing materials by polymer extrusion, drawing of copper wires, continuous stretching of plastic films, artificial fibers, hot rolling, wire drawing, glass fiber, metal extrusion and metal spinning, film condensation etc. After the pioneering work by Sakiadis (1961), a large amount of literature is available on boundary layer flow of

Newtonian and non-Newtonian fluids over linear and nonlinear stretching surfaces (Grubka and Bobba, 1985; Andersson, 1992; Yurusoy and Pakdemirli, 1997, 1999; Nadeem et al., 2010; Rana and Bhargava, 2012; Hady et al., 2012; Qasim et al., 2013). The problem of laminar fluid flow which results from the stretching of a flat surface in a nanofluid was investigated numerically by Khan and Pop (2010). Hassani (2011) investigated the boundary layer flow problem of a nanofluid past a stretching sheet analytically by using the Homotopy Analysis Method. Both the effect of Brownian motion and thermophoresis were considered simultaneously in this case. A numerical investigation on boundary layer flow induced in a nanofluid due to a linearly stretching sheet in the presence of thermal radiation and induced magnetic field was conducted by Gbadeyan et al. (2011).

Later on studies over convective heat transfer of nanofluids gained too much interest due to its application in various industrial processes. A study on free convective flow over a vertical stretching surface was conducted by Wang (1989). Makinde and Ogulu (2008) have examined the effects of thermal radiation on heat and mass transfer of a variable viscosity fluid permeated with a uniform magnetic field. Kuznetsov and Nield (2010) have examined the influence of nanoparticles on natural convection boundary-layer flow past a vertical plate, using a model in which Brownian motion and thermophoresis are taken into account. The authors have assumed the simplest possible boundary conditions, namely those in which both the temperature and the nanoparticle fraction are constant along the wall. Further, Nield and Kuznetsov (2007) have studied the Cheng and Minkowycz (1977) problem of natural convection past a vertical plate, in a porous medium saturated by a nanofluid. The model used for the nanofluid incorporates the effects of Brownian motion and thermophoresis. The study of internal heat generation or absorption is important in problems involving chemical reactions where heat may be generated or absorbed. Studies involving internal heat generation include those of Sparrow and Cess (1962), Anjalidevi and Kandasamy (1999) gave an approximate solution for the steady laminar flow along a semi innite horizontal plate in the presence of species concentration and chemical reaction using numerical technique. Makinde (2009) investigated the magnetic field on boundary layer flow and mass transfer past a vertical plate in a porous medium with constant heat flux.

However, only a limited attention has been paid to the study of effect of chemical reaction over stretching surfaces which is useful in many industrial applications processes such as manufacturing of ceramics, food processing and polymer production, drying, evaporation, energy transfer in a cooling tower and the flow in a desert cooler, heat and mass transfer occur simultaneously. Kameswaran et al. (2012) investigated the convective heat and mass transfer in nanofluid flow over a stretching sheet when subjected to hydromagnetic, viscous dissipation, chemical reaction and Soret effects. Roshima et al. (2011) theoretically studied the problem of steady boundary-layer flow of a nanofluid past a porous stretching surface with variable stream conditions and chemical reaction. Rosca et al. (2012) have studied the steady forced convection stagnation point-flow and mass transfer past a permeable stretching/shrinking sheet placed in a copper (Cu)-water based nanofluid. Many branches of science and engineering such as in nuclear reactor safety, combustion systems, solar collectors, metallurgy, nuclear reactor cooling systems, biomedicine, electronics, glass fiber, hot rolling, food and transportation and chemical engineering joint action of the buoyancy forces from both thermal and mass diffusion show the importance of internal heat generation or absorption with chemical reaction. Motivated by the above work author's prime objective is to study the effect of chemical reaction on stagnation point flow and heat transfer over a stretching surface of a nanofluid in the presence of non uniform heat source/sink in the region of uniform magnetic field. This is achieved by solving transformed non-linear boundary layer equations using appropriate numerical technique Runge–Kutta–Fehlberg 45 method with the help of an algebraic software MAPLE. Variations of several pertinent emerging parameters are to be analyzed in detail.

2. Mathematical Formulation

Consider a steady, incompressible, laminar, two-dimensional boundary layer flow of nanofluid past a vertical strething sheet. The flow is considered along the $x-$axis, which is taken along the vertical sheet in the upward direction, and the $y-$axis is taken normal to it. Keeping the origin fixed, the sheet is then stretched with a velocity $U_w(x)$, varying nonlinearly with the distance from the slit. It is assumed that at the stretching surface, the temperature T and the nanoparticle fraction C take constant values T_w and C_w respectively. The ambient values, attained as y tends to infinity, of T and C are denoted by T_1 and C_1, respectively. The basic steady conservation of mass, momentum, thermal energy and nanoparticles equations for nanofluids in presence of uniform magnetic field can be written in Cartesian coordinates x and y as, (Choi, 1995; Qasim et al., 2013; Hassani et al., 2011),

$$\frac{\partial u}{\partial x}+\frac{\partial v}{\partial y}=0, \tag{2.1}$$

$$u\frac{\partial u}{\partial x}+v\frac{\partial u}{\partial y}=-\frac{1}{\rho}\frac{dP}{dx}+\nu\frac{\partial^2 u}{\partial y^2}-\frac{\sigma B_0^2}{\rho}u\pm(1-C_\infty)\rho_{f\infty}\beta g(T-T_\infty)\pm(\rho_P-\rho_{f\infty})g(C-C_\infty), \tag{2.2}$$

$$u\frac{\partial T}{\partial x}+v\frac{\partial T}{\partial y}=\alpha_m\frac{\partial^2 T}{\partial y^2}+\tau\left[D_B\frac{\partial C}{\partial y}\frac{\partial T}{\partial y}+\frac{D_T}{T_\infty}\left(\frac{\partial T}{\partial y}\right)^2\right]+q''', \tag{2.3}$$

$$u\frac{\partial C}{\partial x}+v\frac{\partial C}{\partial y}=D_B\frac{\partial^2 C}{\partial y^2}+\frac{D_T}{T_\infty}\frac{\partial^2 T}{\partial y^2}-k_1C. \tag{2.4}$$

In (2.2) "+" sign corresponds to an assisting flow and "-" refers to an opposing flow and q''' is expressed as

$$q'''=\frac{K^*U_w(x)}{x\upsilon},\left[A_1(T_w-T_\infty)f'(\eta)+(T-T_\infty)B_1\right] \tag{2.5}$$

Here we make a note that the case $A_1>0$, $B_1>0$ corresponds to internal heat generation and $A_1<0$, $B_1<0$ corresponds to internal heat absorption.

The respective boundary conditions are given by:

$$\begin{aligned}&u=U_w(x),\quad v=-V_w(x),\quad T=T_w,\quad C=C_w,\quad \text{at } y=0,\\ &u=U(x),\quad v=0,\quad T\to T_\infty,\quad C\to C_\infty,\quad \text{as } y\to\infty.\end{aligned} \tag{2.6}$$

Equations (2.1)-(2.4) subjected to boundary condition (2.6), admit the locally similar solution in terms of the similarity function f and the similarity variable η defined by

$$\begin{aligned}&u=cxf'(\eta),\quad v=\sqrt{c\upsilon}\,f(\eta),\quad \eta=\sqrt{\frac{c}{\upsilon}}\,y,\\ &\theta=\frac{T-T_\infty}{T_w-T_\infty},\quad \phi=\frac{C-C_\infty}{C_w-C_\infty},\end{aligned} \tag{2.7}$$

where a prime denotes the differentiation with respect to η. Substituting (2.7) into equations (2.1)-(2.4) one obtains

$$f'''(\eta)+f(\eta)f''(\eta)-f'(\eta)^2+A^2-Q(f'(\eta)-A)\pm Ra_x(\theta+Nr\phi)=0, \tag{2.8}$$

$$\theta''(\eta)\frac{1}{\mathrm{Pr}}+f(\eta)\theta'(\eta)+\phi'(\eta)\theta'(\eta)Nb+Nt(\theta'(\eta))^2+A_1f'(\eta)+B_1\theta(\eta)=0, \tag{2.9}$$

$$\phi''(\eta)+Lef(\eta)\phi'(\eta)+\frac{Nt}{Nb}\theta''(\eta)-\gamma\phi(\eta)=0. \tag{2.10}$$

The transformed boundary conditions are given by

$$\begin{aligned}&f'(\eta)=1,\quad f(\eta)=f_0,\quad \theta(\eta)=1,\quad \phi(\eta)=1,\quad \text{at } \eta=0,\\ &f'(\eta)=\frac{b}{c},\quad \theta(\eta)=0,\quad \phi(\eta)=0,\quad \text{as } \eta\to\infty.\end{aligned} \tag{2.11}$$

In deriving these equations, the external electric field is assumed to be zero and the electric field due to polarization of charges is negligible.

3. Numerical solution

The equations (2.8), (2.9) and (2.10) together with the boundary condition (2.11) forms highly non-linear ordinary differential equations. In order to solve these nonlinear equations a symbolic software Maple has been adopted, which is very efficient in using the well known Runge-Kutta-Fehlberg fourth-fifth order method. This algorithm in MAPLE has been well tested for its accuracy and robustness. As it is a boundary value problem, an appropriate method needs to be selected. The available sub-method in MAPLE 12.0 is the combination of base schemes; trapezoidal and midpoint method. In these two major considerations, trapezoidal method is generally efficient for typical problems, but the midpoint method is so capable of handling harmless end-point singularities that the trapezoid method cannot. The midpoint method, also known as fourth-fifth order Runge-Kutta-Fehlberg method, improves the Euler method by adding a midpoint in the step which increases the accuracy by one order. In this regard the midpoint method is used as a suitable numerical technique. In accordance with the boundary layer analysis, the boundary condition (2.11) at $\eta=\infty$ were replaced by $\eta=5$.

Accuracy of this numerical method is being validated by direct comparison with the numerical results reported by Khan and Pop (2010), Wang (1989) and Rosmila et al. (2011) with $A_1=B_1=Nr=0$.

Table-1: Comparative results of $-\theta'(0)$ for various values of Pr with $A_1 = B_1 = Nr = 0$.

Pr	Khan and Pop (2010)	Wang (1989)	Rosmila et al. (2011)	Present result
0.72	0.4539	0.4539	0.4530	0.4540
2	0.9113	0.9114	0.9114	0.9113
7	1.8954	1.8954	1.8954	1.8954
20	3.3539	3.3539	3.3539	3.3539
70	6.4621	6.4622	6.4622	6.4622

Table 2 and 3 are inferred to show the effect of physical parameters on skin friction coefficient, Nusselt number and Sherwood number for the case of assisting and opposing flows. It is observed that in both the cases for the skin friction co-efficient $(f''(0))$ and Sherwood number $(-\phi'(0))$ respond positively for the increasing values of $\Pr, Le, A_1, B_1, Q, f_0, A$. Whereas, Nusselt number $(-\theta'(0))$ respond negatively for increasing value of these physical parameters. This is due to the fact that temperature gradient is minimum in the region because thermal boundary layer thickness in the region becomes very large, accompanied by a reduction in the temperature gradient.

4. Results and Discussion

The boundary layer problem for momentum, heat and mass transfer with space for a nanofluid flow along with chemical reaction effect over a stretching sheet in the presence of non-uniform heat source/sink is examined in this paper. The respective profiles for the both assisting and opposing flows are depicted graphically. The computation through employed numerical scheme (RKF-45 method) has been carried out for various values of the flow parameters such as magnetic parameter (Q), chemical reaction parameter (γ), Prandtl number $(\Pr)$, nonuniform heat source (A_1 and B_1), Lewis number (Le), Brownian motion (Nb), thermophoresis parameter (Nt) and bouyancy ratio (Nr).

Figures 1(a) and 1(b) depict temperature profile (θ) and concentration profile (ϕ), for different values of Prandtl number $(\Pr)$ for both the opposing and assisting flows. One can find that temperature of nanofluid particles decreases with the increase in Pr which implies viscous boundary layer is thicker than the thermal boundary layer. The temperature asymptotically approaches to zero in the free stream region.

Figures 2(a) and 2(b) presents typical profile for temperature and concentration for various values of thermophoretic parameter (Nt) for both opposing and assisting flows. It is observed that in both the cases an increase in the thermophoretic parameter leads to increase in fluid temperature and nanoparticle concentrations. This thermophoresis serves to warm the boundary layer for low values of Pr and Lewis number (Le).

Table-2: Wall temperature gradient $-\theta'(0)$, $f''(0)$ and $-\phi'(0)$ for the case of assisting flow for different values of the parameters $\Pr, Le, Nt, Nb, Nr, A_1, B_1, Q, f_0, A$ and γ.

Nt	Nb	Nr	Q	f_0	A_1	B_1	Pr	Le	γ	A	$-\theta'(0)$	$f''(0)$	$-\phi'(0)$
0.5	0.5	0.5	3	0.02	0.002	0.002	0.72	10	1	1	0.4287	-0.4370	2.8962
1											0.4397	-0.3733	2.9686
2											0.4562	-0.2795	3.1633
0.5	0.5	0.5	3	0.02	0.002	0.002	0.72	10	1	1	0.4287	-0.4370	2.8962
	1										0.4345	-0.3191	2.9226

Table-2 (continued): Wall temperature gradient $-\theta'(0)$, $f''(0)$ and $-\phi'(0)$ for the case of assisting flow for different values of the parameters Pr, Le, Nt, Nb, Nr, A_1, B_1, Q, f_0, A and γ.

Nt	Nb	Nr	Q	f_0	A_1	B_1	Pr	Le	γ	A	$-\theta'(0)$	$f''(0)$	$-\phi'(0)$
	2										0.4461	-0.1671	2.9209
0.5	0.5	0.5	3	0.02	0.002	0.002	0.72	10	1	1	0.4287	-0.4370	2.8962
		1									0.5113	-0.4382	2.9029
		2									0.6756	-0.4405	2.9160
0.5	0.5	0.5	3	0.02	0.002	0.002	0.72	10	1	1	0.4287	-0.4370	2.8962
			2								0.4578	-0.4386	2.9009
			1								0.4947	-0.4406	2.9070
0.5	0.5	0.5	3	0.02	0.002	0.002	0.72	10	1	1	0.4287	-0.4370	2.8962
				0.5							0.4008	-0.5738	6.3992
				1							0.3791	-0.07336	10.6686
0.5	0.5	0.5	3	0.02	-0.04	0.002	0.72	10	1	1	0.4218	-0.4740	2.8865
					0						0.4283	-0.4388	2.8957
					0.04						0.4349	-0.4030	2.9051
0.5	0.5	0.5	3	0.02	0.002	-0.5	0.72	10	1	1	0.4118	-0.6041	2.8108
						0					0.4286	-0.4378	2.8958
						0.5					0.4523	-0.2293	2.9928
0.5	0.5	0.5	3	0.02	0.002	0.002	0.72	10	1	1	0.4287	-0.4370	2.8962
							2				0.4280	-0.3850	2.2579
							3				0.4245	-0.2950	2.3523
0.5	0.5	0.5	3	0.02	0.002	0.002	0.72	1	1	1	0.4902	-0.4833	0.4902
								5			0.4498	-0.4486	2.1234
								10			0.4287	-0.4370	2.8962
0.5	0.5	0.5	3	0.02	0.002	0.002	0.72	10	0.5	1	0.4298	-0.4375	2.8096
									5		0.4212	-0.4340	3.5218
									10		0.4144	-0.4314	4.1824
0.5	0.5	0.5	3	0.02	0.002	0.002	0.72	10	1	0.5	0.6040	-1.6174	0.3258
										1	0.4144	-0.4314	2.1824
										1.5	1.6762	-0.5074	2.2550

Table-3: Wall temperature gradient $-\theta'(0)$, $f''(0)$ and $-\phi'(0)$ for the case of opposing flow for different values of the parameters Pr, Le, Nt, Nb, Nr, G, A_1, B_1, Q, f_0, A and γ.

Nt	Nb	Nr	Q	f_0	A_1	B_1	Pr	Le	γ	A	$-\theta'(0)$	$f''(0)$	$-\phi'(0)$
0.5	0.5	0.5	3	0.02	0.002	0.002	0.72	10	1	1	0.4423	-0.4101	2.7904
1											0.4541	-0.3486	2.8546

Table-3 (continued): Wall temperature gradient $-\theta'(0)$, $f''(0)$ and $-\phi'(0)$ for the case of opposing flow for different values of the parameters Pr, Le, Nt, Nb, Nr, G, A_1, B_1, Q, f_0, A and γ.

Nt	Nb	Nr	Q	f_0	A_1	B_1	Pr	Le	γ	A	$-\theta'(0)$	$f''(0)$	$-\phi'(0)$
2											0.4716	-0.2588	3.0305
0.5	0.5	0.5	3	0.02	0.002	0.002	0.72	10	1	1	0.4423	-0.4101	2.7904
	1										0.4484	-0.2988	2.8136
	2										0.4608	-0.1558	2.8080
0.5	0.5	0.5	3	0.02	0.002	0.002	0.72	10	1	1	0.4423	-0.4101	2.7904
		1									0.5297	-0.4087	2.7823
		2									0.7061	-0.4058	2.7659
0.5	0.5	0.5	3	0.02	0.002	0.002	0.72	10	1	1	0.4423	-0.4101	2.7904
			2								0.4765	-0.4080	2.7841
			1								0.5224	-0.4051	2.7754
0.5	0.5	0.5	3	0.02	0.002	0.002	0.72	10	1	1	0.4423	-0.4101	2.7904
				0.5							0.4014	-0.5524	6.3354
				1							0.3863	-0.7168	10.6316
0.5	0.5	0.5	3	0.02	-0.04	0.002	0.72	10	1	1	0.4350	-0.4462	2.7839
					0						0.4419	-0.4118	2.7903
					0.04						0.4489	-0.3771	2.7965
0.5	0.5	0.5	3	0.02	0.002	-0.5	0.72	10	1	1	0.4424	-0.5877	2.7068
						0					0.4422	-0.4109	2.7900
						0.5					0.4725	-0.1767	2.8865
0.5	0.5	0.5	3	0.02	0.002	0.002	0.72	10	1	1	0.4423	-0.4101	2.7904
							2				0.4179	-0.3303	2.9478
							3				0.4141	-0.2382	3.0407
0.5	0.5	0.5	3	0.02	0.002	0.002	0.72	1	1	1	0.5066	-0.4441	1.2085
								5			0.4650	-0.4190	2.0385
								10			0.4423	-0.4101	2.7904
0.5	0.5	0.5	3	0.02	0.002	0.002	0.72	10	0.5	1	0.4436	-0.4105	2.6985
									5		0.4336	-0.4075	3.4455
									10		0.4259	-0.4053	4.1256
0.5	0.5	0.5	3	0.02	0.002	0.002	0.72	10	1	0.5	1.6174	-0.3258	1.8603
										1	0.4259	-0.4053	2.1256
										1.5	0.8315	-0.4871	2.1913

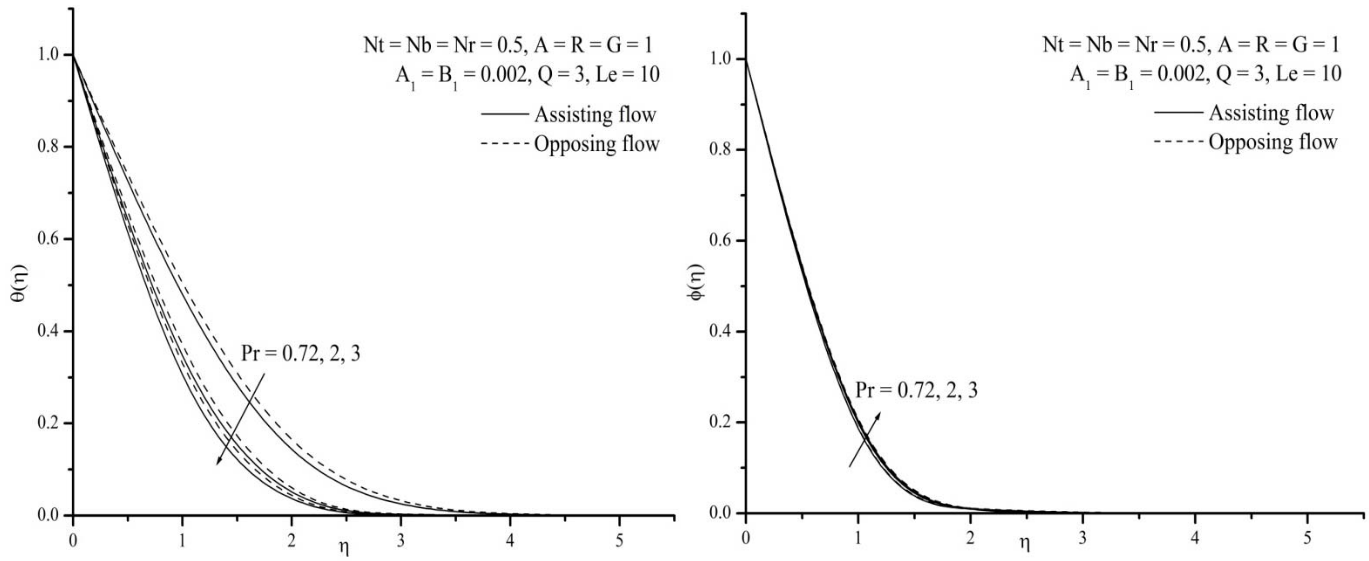

Figure 1(a) & 1(b): Effect of Prandtl number $(\Pr)$ on temperature and concentration profiles.

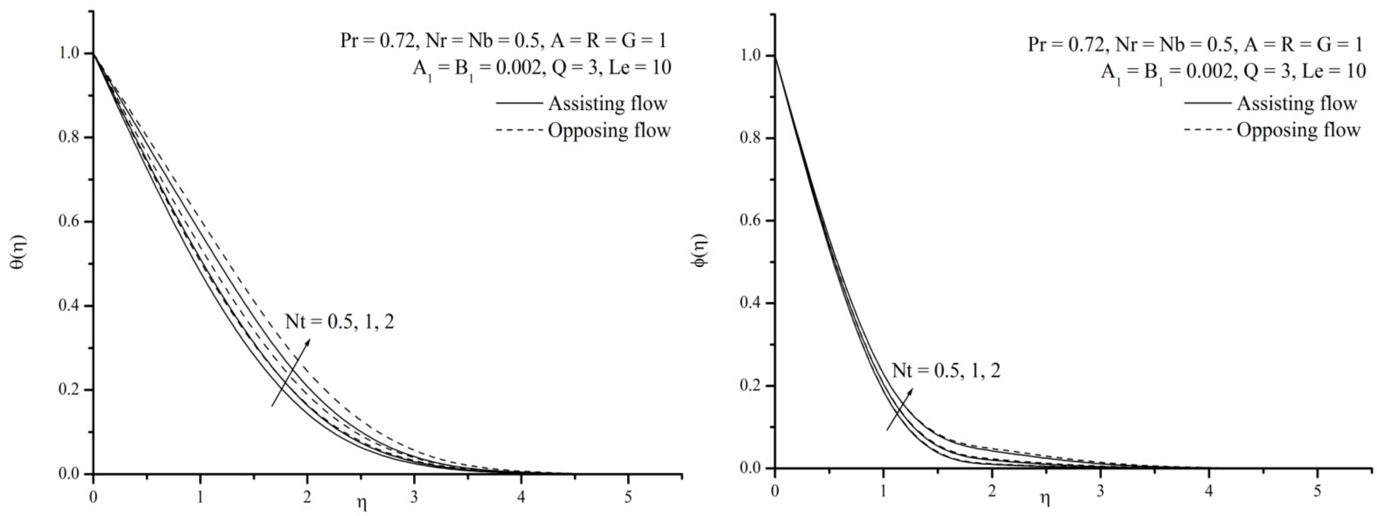

Figure 2(a) & 2(b): Effect of thermophoresis parameter (Nt) on temperature and concentration profiles.

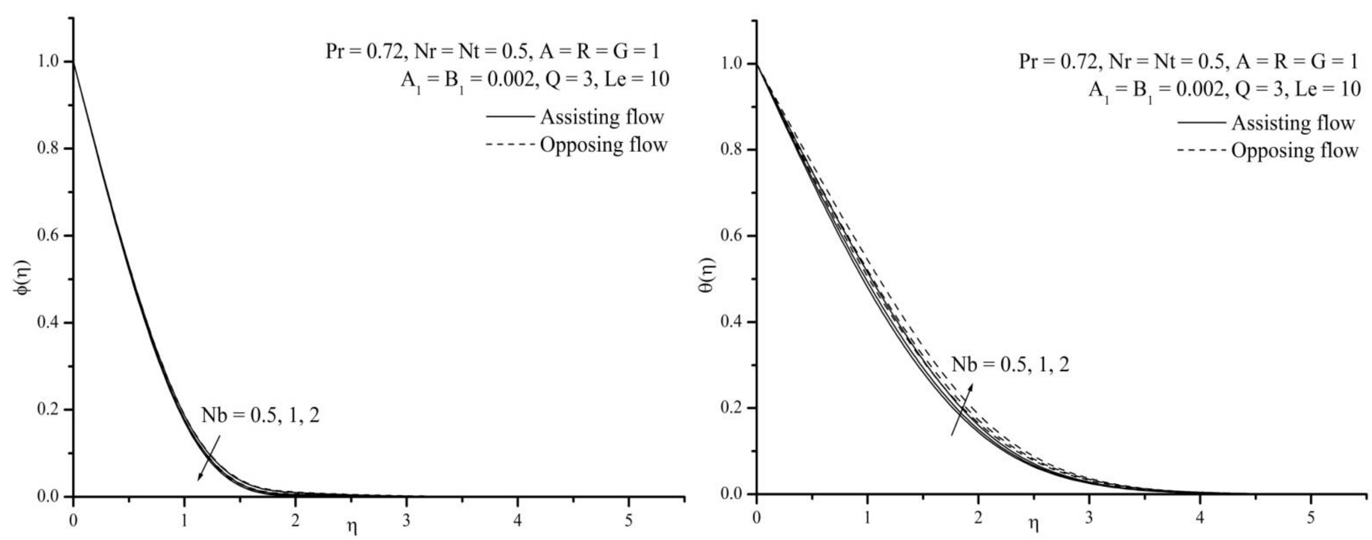

Figure 3(a) & 3(b): Effect of Brownian motion parameter (Nb) on temperature and concentration profiles.

The effect of Brownian motion parameter (Nb) on temperature and concentration profiles for both the assisting and opposing flows are shown in figures 3(a) and 3(b). As expected, the boundary layer profiles for the temperature are of the same form as in the case of regular heat transfer fluids. Temperature in the boundary layer increases and the nanoparticle volume fraction decreases with the increase in Brownian motion parameter. Brownian motion serves to warm the boundary layer and simultaneously exacerbates particle deposition away from the fluid regime or onto the surface, thereby accounting for the reduced concentration magnitudes. For small particles, Brownian motion is strong and the parameter Nb will have high values, the converse is the case for large particles and clearly Brownian motion does exert a significant enhancing influence on both temperature and concentration profiles.

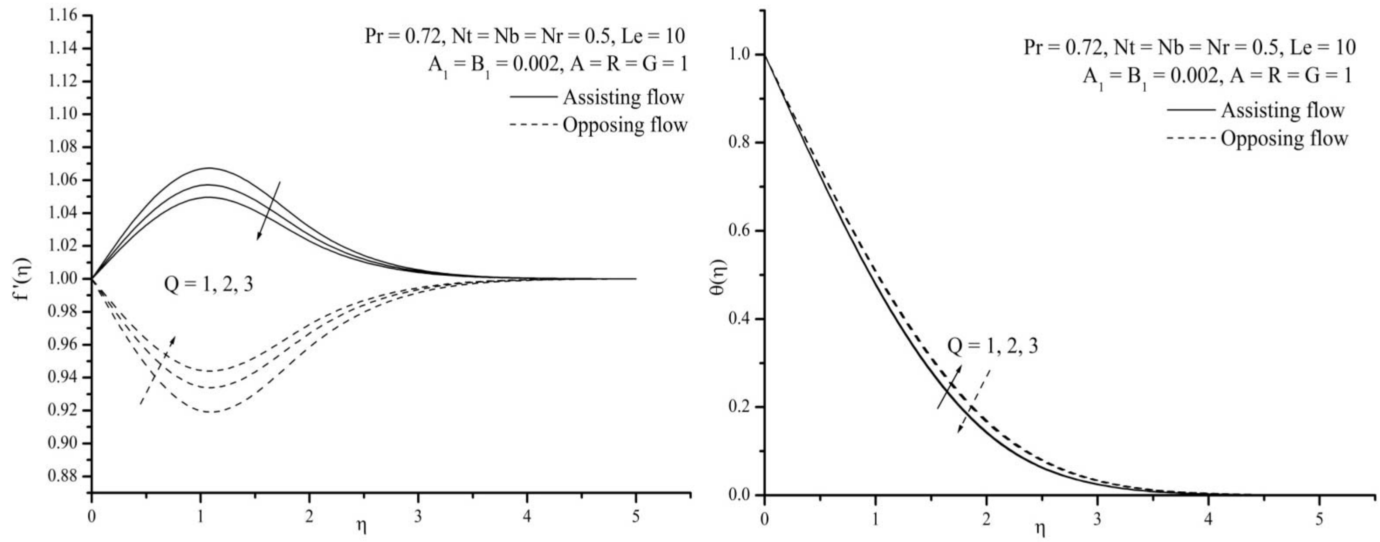

Figure 4(a) & 4(b): Effect of magnetic parameter (Q) on velocity and temperature profiles.

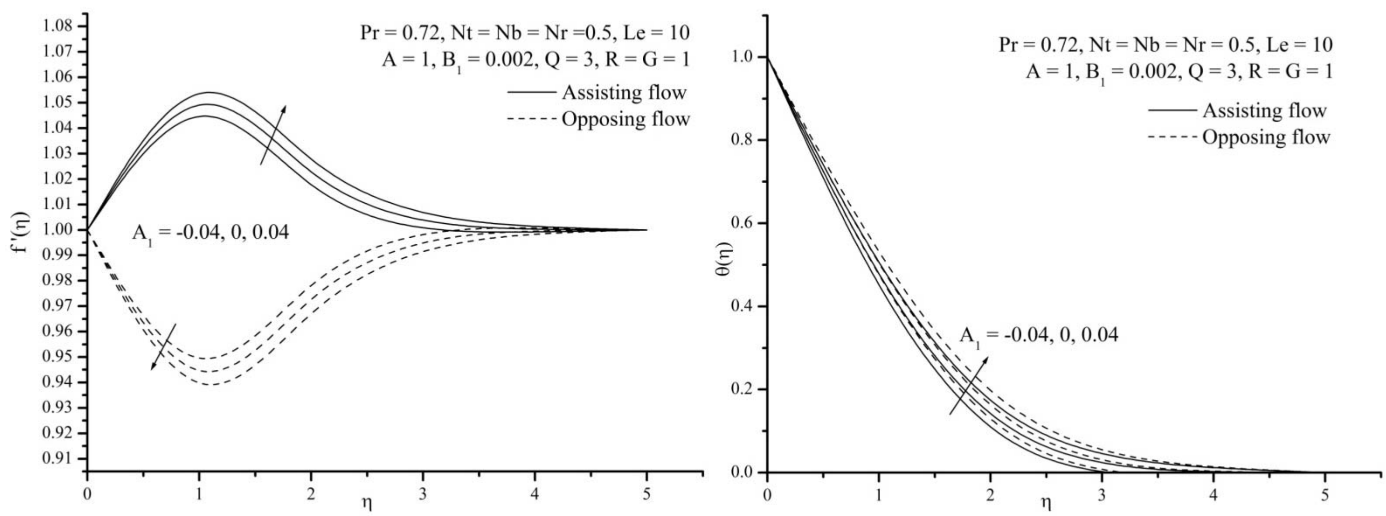

Figure 5(a) & 5(b): Effect of source/sink parameter (A_1) on velocity and temperature profiles.

From the figures 4(a) and 4(b), it is noticed that the velocity (f') along the surface decreases for the case of assisting flow but increases in the case of opposing flow, while the temperature increases with the magnetic parameter (Q). Thus the presence of magnetic field decreases the momentum boundary layer thickness and increases the thermal boundary layer thickness. It is also observed that, for a specific value of Q and at each position, the corresponding values for the velocity of pure fluid and the temperature are different.

In figures 5(a) and 5(b), the effects of heat source/sink (A_1) on velocity and temperature distributions for both the assisting and opposing flows are shown. The term A_1 is assumed to be the amount of heat generated/absorbed per unit volume. When the wall temperature exceeds the free stream temperature, the source term represents the heat source for $A_1 > 0$ and heat sink for $A_1 < 0$ whereas $T_w < T_1$. Opposite of the preceding relationship is also true. The presence of heat source in the boundary layer generates energy which causes the velocity and the temperature of the fluid to increase. This increase in temperature produces an increase in the flow field. This is caused due to the buoyancy effect of both pure water and nanofluid but the effect is more pronounced in case of nanofluids as shown in figure. On the other hand, the presence of heat sink in the boundary layer absorbs energy which causes the velocity and the temperature of the fluid to decrease. Figures 6(a) and 6(b) are graphical representations of velocity and temperature distributions source/sink parameter (B_1). Predictions of B_1 are similar to that of A_1.

Figure 7 shows the effect of chemical reaction $(\gamma = G)$ on nanoparticle concentration profile for both the assisting and opposing flows. It is seen that the nanoparticle volume fraction of the fluid decreases with increase of chemical reaction parameter γ, while the velocity and temperature profiles are found to be insignificant for the increasing value of chemical reaction parameter. In particular, the nanoparticle volume fraction of the fluid gradually changes from higher value to the lower value only when the strength of the chemical reaction is higher than the thermophoresis particle deposition. For nanoparticle volume characteristics mechanism, interesting result is the large distortion of the nanoparticle volume field. All these physical behavior are due to the combined effects of the strength of the Brownian motion and thermophoresis particle deposition.

Figures 8(a) and 8(b) depict the variation of temperature and concentration with coordinate for various values of Lewis numbers (Le) for both the assisting and opposing flows. The thickness of the boundary layer concentration is found to be smaller than the thermal boundary layer thickness for $Le > 1$. Both the temperature and concentration profiles decrease with an increase in Lewis number. But, the concentration profile is affected more even for small value of Le as compared to temperature profile. Also, the concentration and thermal layers will be reduced in thickness compared with the velocity boundary layer.

Figure 9 shows the temperature profile of the bouyancy ratio (Nr) for both the assisting and opposing flows. It is observed that the increase in the value of Nr produces a significant increases in the thickness of the thermal boundary layer of the nanofluid. So, the temperature distribution increases with the increasing value of Nr in the case of opposing flow but reverses the situation in the case of opposing flow.

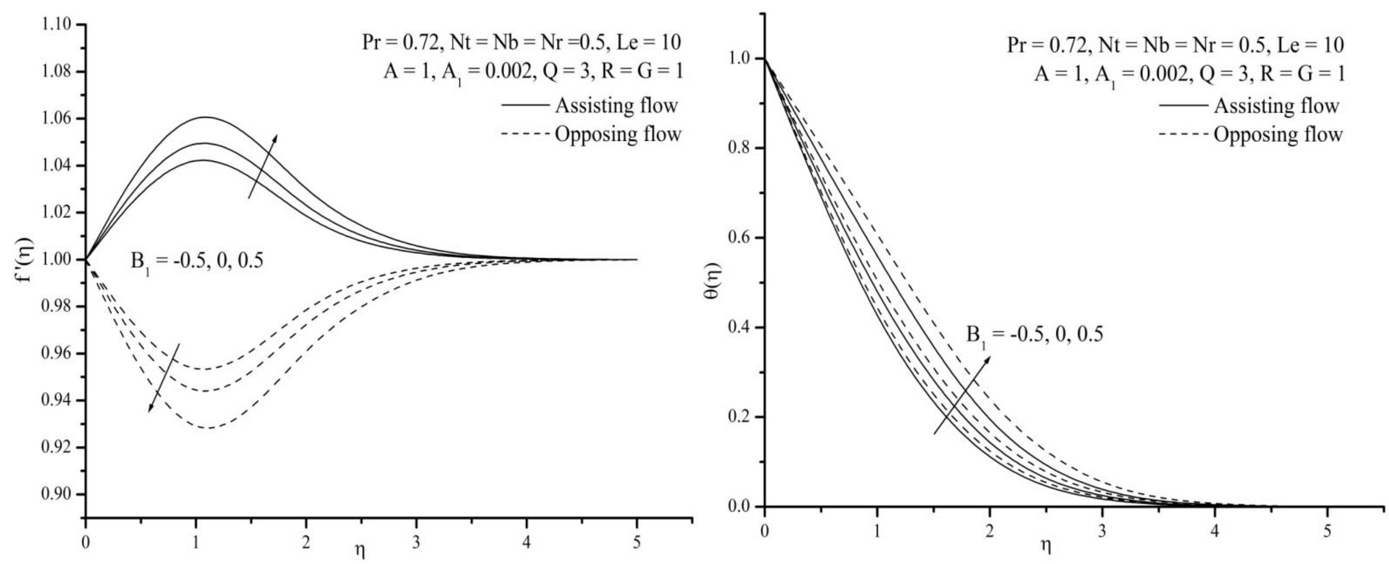

Figure 6(a) & 6(b): Effect of source/sink parameter (B_1) on velocity and temperature profiles.

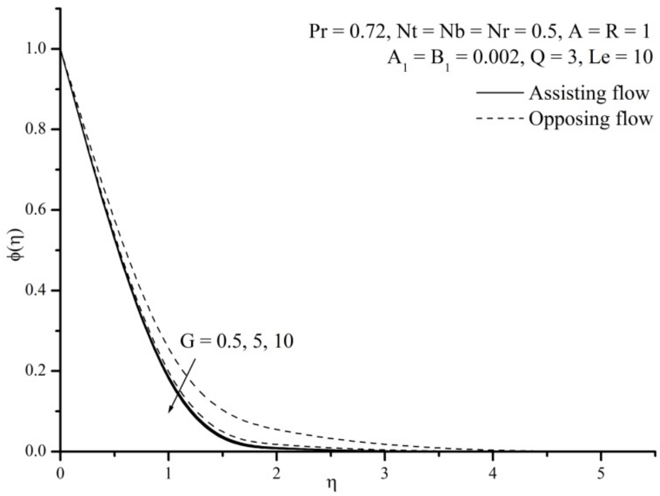

Figure 7: Effect of chemical reaction parameter $(G = \gamma)$ on concentration profile.

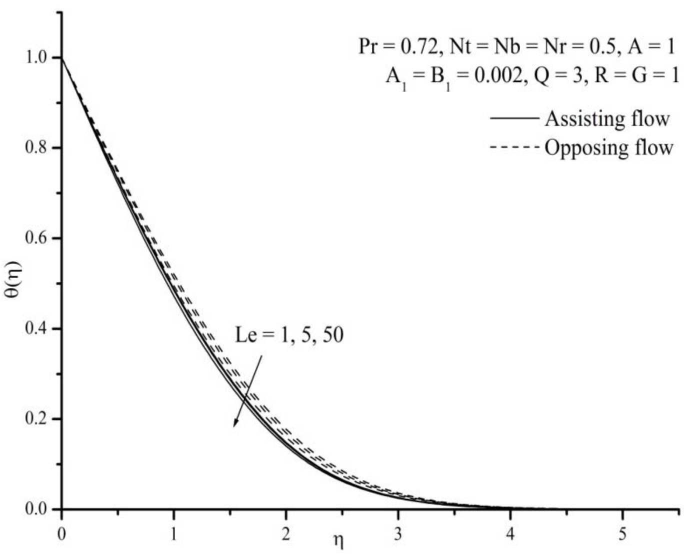

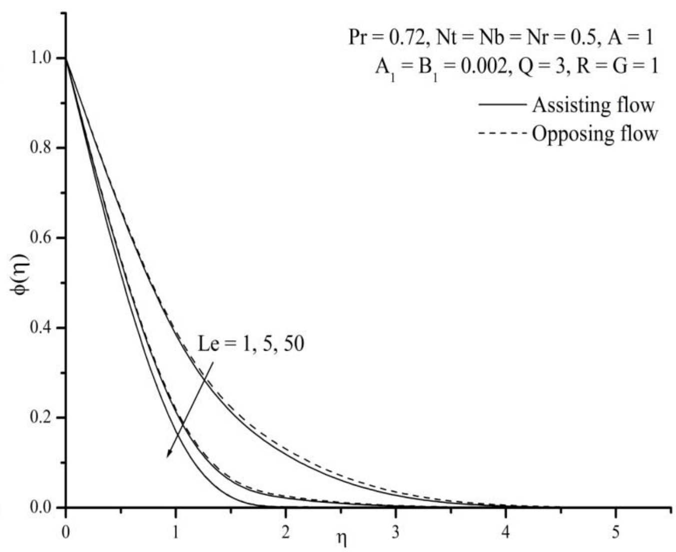

Figure 8(a) & 8(b): Effect of Lewis number (Le) on temperature and concentration profiles.

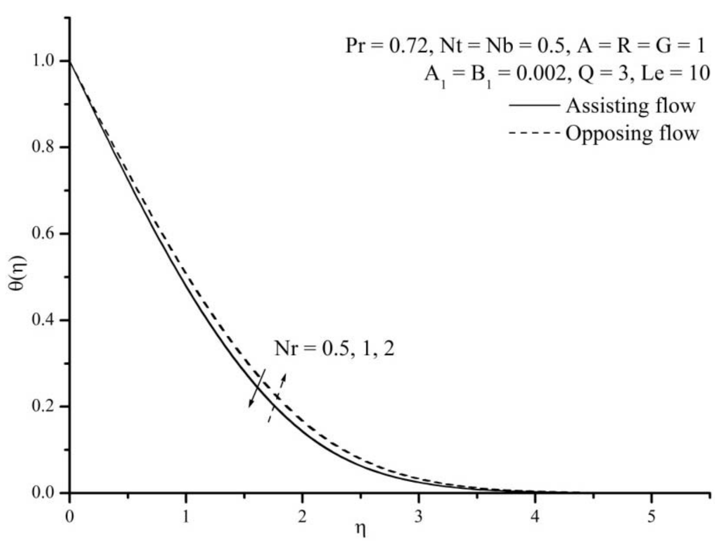

Figure 9: Effect of bouyancy ratio (Nr) on the temperature profile.

5. Conclusions

Under the assumption of thermophoresis particle deposition, the present investigation reflects theoretically the effect of chemical reaction on stagnation point flow of a nanofluid over a vertical stretching sheet in the presence of non-uniform heat source/sink and uniform magnetic field. The results pertaining to the present study indicate, that

- The effect of Prandtl number is to decrease the thermal boundary layer thickness, which is in contrast to the effects of other parameter on heat transfer.
- The magnetic field suppresses the velocity field of the nanofluid, which in turn causes the enhancement of the temperature field.
- The impact of the heat source with thermophoresis particle deposition in the presence of magnetic field have a substantial effect on the flow field and thus, on the heat and mass transfer rate from the sheet to the fluid.
- The concentration boundary layer is significantly suppressed by the thermophoretic force and the effect of thermophoresis plays a dominant role than that of diffusion, thus almost uniform deposition efficiency is achieved for clusters of different sizes.
- For the value of Lewis number thickness of the boundary layer concentration is found to be smaller than the thermal boundary layer thickness.
- Increasing values of bouyancy ratio produces a significant increase in the thickness of thermal boundary layer.
- Increase in the strength of chemical reaction parameter result in the large distortion of the nanoparticle volume field. This effect of thermophoresis particle deposition with chemical reaction plays an important role on the rapid growth of World's economy, has led to severe air pollution characterized by acid rain, severe pollution in cities, and regional air pollution.

The results of the problem are also of great interest in a melt-spinning process, the extrudate from the die is generally drawn and simultaneously stretched into a filament or sheet, which is thereafter solidified through rapid quenching or gradual cooling by direct contact with water or chilled metal rolls.

Nomenclature

(u,v)	velocity components along the x and y axes
ρ	density of the nanofluid,
α_m	thermal diffusivity
υ	kinematic viscosity
D_B	Brownian diffusion coefficient
D_T	thermophoresis diffusion coefficient
T	nanofluid temperature
P	nanofluid pressure
B_0	induced magnetic field
$\tau = \frac{(\rho c)_p}{(\rho c)_f}$	ratio between the effective heat capacity of the nanoparticle material and heat capacity of the fluid
C	volumetric volume expansion coefficient
ρ_p	density of the nanoparticles
$\rho_{f\infty}$	density of the nanoparticle in the free stream region
g	acceleration due to gravity
k_1	rate chemical reaction
T_w	temperature of the nanofluid near wall
T_∞	free stream temperature of the nanofluid
A_1 , B_1	coefficient of space and temperature dependent heat source/sink
K^*	thermal conductivity
q'''	space and temperature dependent internal heat generation/absorption (non-uniform heat ource/sink)
$U_w(x) = cx$	stretching sheet velocity
$U(x) = bx$	free stream velocity

$V_w(x) = f_0\sqrt{\upsilon c}$ suction velocity

c stretching rate being a positive constant

$A = \dfrac{b}{c}$ ratio of free stream velocity parameter to stretching sheet parameter

$Q = \dfrac{\sigma B_0^2}{\rho c}$ magnetic parameter

$Ra_x = \dfrac{(1 - C_\infty)\beta g(T_w - T_\infty)f_\infty}{c^2 x}$ local Rayleigh number

$Nr = \dfrac{(\rho_P - \rho_{f_\infty})\beta g(C_w - C_\infty)f_\infty}{\rho_{f_\infty}\beta(T_w - T_\infty)(1 - C_\infty)}$ buoyancy ratio

$\Pr = \dfrac{\upsilon}{\alpha_m}$ Prandtl number

$Nt = \dfrac{\tau D_T(T_w - T_\infty)}{\upsilon T_\infty}$ thermophoresis parameter

$N_B = \dfrac{\tau D_B(C_w - C_\infty)}{\upsilon}$ Brownian motion parameter,

$Le = \dfrac{\upsilon}{D_B}$ Lewis number,

$\gamma = \dfrac{k_1 U(C_w - C_\infty)}{\upsilon}$ chemical reaction parameter.

Acknowledgement: The authors are very much thankful to the reviewers for their constructive suggestions to improve the quality of the article.

References

Andersson H.I., 1992, MHD flow of a visco-elastic fluid past a stretching sheet, Acta Mech., Vol.95, pp.227-230.

Anjalidevi S.P. and Kandasamy R., 1999, Effects of chemical reaction heat and mass transfer on laminar flow along a semi-infinite horizontal plate, Heat and Mass Transfer,Vol.35, pp.465-467.

Buongiorno J. and Hu W., 2005, Nanofluid coolants for advanced nuclear power plants”. Proceedings of ICAPP 05: Seoul. Sydney: Curran Associates, Inc., pp.15-19.

Buongiorno J., 2005, Convective transport in nanofluids, ASME J. Heat Trans., Vol.128, pp.240-250.

Cheng P. and Minkowycz W.J., 1977, Free convection about a vertical flat plate embedded in a porous medium with application to heat transfer from a dike, J. Geophysics Research, Vol.82, No.14, pp.2040-2044.

Choi S.U.S., 1995, Enhancing thermal conductivity of fluids with nanoparticle, In: D.A. Siginer, H.P. Wang (Eds.), Developments and Applications of Non-Newtonian Flows, The ASME New York. FED Vol.231/MD Vol.66, pp. 99-105.

Dae-Hwang Yoo, Hong K.S. and Ho-Soon Yang, 2007a, Study of thermal conductivity of nanofluids for the application of heat transfer fluids, Thermochimica Acta, Vol.455, No.1–2, pp.66–69.

Dae-Hwang Yoo, Hong K.S., Hong T.E., Eastman J.A. and Ho-Soon Yang, 2007b, Thermal conductivity of Al_2 O_3/water nanofluids, J. Korean Phy. Society, Vol.51, pp.S84-S87.

Fan J. and Wang L., 2011, Heat conduction in nanofluids: structure-property correlation, Int. J. Heat Mass Trans. Vol.54, pp.4349-4359.

Fekry M. Hady, Fouad S. Ibrahim, Sahar M. Abdel-Gaied and Mohamed R. Eid, 2012, Radiation effect on viscous flow of a nanofluid and heat transfer over a nonlinearly stretching sheet, Nanoscale Research Letters, Vol.7, pp.229.

Gbadeyan J.A., Olanrewaju M.A. and Olanrewaju P.O., 2011, boundary layer flow of a nanofluid past a stretching sheet with a convective boundary condition in the presence of magnetic field and thermal radiation, Australian J. Basic Applied Sci., Vol.5, No.9, pp.1323-1334.

Grubka L.J. and Bobba K.M., 1985, Heat transfer characteristic of a continuous stretching surface with variable temperature, J. Heat Trans., Vol.107, pp.248-250.

Hassani M., Mohammad Tabar M., Nemati H., Domairry G. and Noori F., 2011, An analytical solution for boundary layer flow of a nanofluid past a stretching sheet, Int. J. Thermal Sc. Vol.50, No.11, pp.2256–2263.

Kameswaran P.K., Narayana M., Sibanda P. and Murthy P.V.S.N., 2012, Hydromagnetic nanofluid flow due to a stretching or shrinking sheet with viscous dissipation and chemical reaction effects, Int. J. Heat Mass Transfer, Vol.55, No. 25-26, pp. 7587-7595.

Khan W.A. and Pop I., 2010, Boundary-layer flow of a nanofluid past a stretching sheet, Int. J. Heat Mass Trans. Vol.53, pp.2477-2483.

Kleinstreuer C. and Feng Y., 2011, Experimental and theoretical studies of nanofluid thermal conductivity enhancement: a review, Nanoscale Research Letters, Vol.6, pp.229.

Kuznetsov A.V. and Nield D.A., 2010, Natural convective boundary-layer flow of a nanofluid past a vertical plate, Int. J. Thermal Sci. Vol.49, No.2, pp.243-247.

Makinde O.D. and Ogulu A., 2008, The effect of thermal radiation on the heat and mass transfer flow of a variable viscosity fluid past a vertical porous plate permeated by a transverse magnetic field, Chem. Eng. Comm., Vol.195, No.12, pp.1575-1584.

Makinde O.D., 2009, On MHD boundary-layer flow and mass transfer past a vertical plate in a porous medium with constant heat flux, Int. J. Numer. Meth. heat fluid flow, Vol.19, pp.546-554.

Masuda H., Ebata A., Teramae K. and Hishinuma N., 1993, Alteration of thermal conductivity and viscosity of liquid by dispersing ultra-fine particles, Netsu Bussei., Vol.7, pp.227-233.

Nadeem S., Hussain A. and Khan M., 2010, HAM solutions for boundary layer flow in the region of the stagnation point towards a stretching sheet, Comm. Nonlinear Sci. Numer. Simul., Vol.15, pp.475-481.

Nield D.A. and Kuznetsov A.V., 2007, The Cheng-Minkowycz problem for natural convective boundary layer flow in a porous medium saturated by a nanofluid, Meccanica, Vol.42, pp.263-272.

Rana P. and Bhargava R., 2012, Flow and heat transfer of a nanofluid over a nonlinearly stretching sheet: A numerical study, Comm. Nonlinear Sci. Numer. Simul., Vol.17, No.1, pp.212–226.

Rosmila Abdul-Kahar, Kandasamy R. and Muhaimin, 2011, Scaling group transformation for boundary-layer flow of a nanofluid past a porous vertical stretching surface in the presence of chemical reaction with heat radiation, Comp. Fluids, Vol.52, No.30, pp. 15-21.

Rosca N.C., Grosan T. and Pop I., 2012, Stagnation-point flow and mass transfer with chemical reaction past a permeable stretching/shrinking sheet in a nanofluid, Sains Malaysiana, Vol.41, No.10, pp.1271–1279.

Sakiadis B.C., 1961, Boundary layer behavior on continuous solid surfaces: I Boundary layer equations for two dimensional and axisymmetric flow, AICHE J. Vol.7, pp.26-28.

Yurusoy M. and Pakdemirli M., 1997, Symmetry reductions of unsteady three-dimensional boundary layers of some non-Newtonian fluids, Int. J. Eng. Sci., Vol.35, No.8, pp.731-740.

Yurusoy M. and Pakdemirli M., 1999, Exact solutions of boundary layer equations of a special non-Newtionian fluid over a stretching sheet, Mech. Res. Comm., Vol.26, No.2, pp.171-175.

Qasim M., Khan I. and Shafie S., 2013, Heat transfer in a micropolar fluid over a stretching sheet with Newtonian heating". PLOS ONE. Vol.8, No.4, pp.1-9.

Wang C.Y., 1989, Free convection on a vertical stretching surface, ZAMM, Vol.69, pp.418-420.

Singh A. K., 2008, Thermal Conductivity of Nanofluids, Defence Sc. J., Vol.58, No.5, pp.600-607.

Sparrow M. and Cess R.D., 1962, Free convection with blowing or suction, J. Heat Transfer, Vol.83, pp.243-248.

Biographical notes

Dr. B.J. Gireesha is a Assistant Professor in the Department of Studies and Research in Mathematics, Kuvempu University, Shankaraghatta-577 451, Shimoga, Karnataka, INDIA. He has more than 14 years of experience in teaching and research. His current area of research includes Fluid Mechanics, and Computer simulation. He has published more than one hundred and ten papers in referred national and international journals. He has also presented more than twenty five research articles in national and international conferences. He has authored and coauthored 3 books. He has successfully completed two major research projects sponsored by Government of India. 7 students are awarded Ph.D., and 11 students are awarded M.Phil., degree under his supervision.

N.G. Rudraswamy is a Research Scholar in the Department of Studies and Research in Mathematics, Kuvempu University, Karnataka, INDIA. His area of interest is nanofluid flow, heat/mass transfer phenomenon, boundary layer theory, numerical simulation. He has two publications to his name in International Journals and two articles in the conference proceedings. He has attended/presented his research articles in two international and four national conferences.

Received October 2013
Accepted April 2014
Final acceptance in revised form July 2014